31st Annual International Conference of the IEEE EMBS
Minneapolis, Minnesota, USA, September 2-6, 2009

Enhanced Susceptibility to Alternans in a Rabbit Model of Chronic Myocardial Infarction

Qing Lou, Igor R. Efimov, PhD

Abstract— **The aim of this study is to examine how structural discontinuity and functional remodeling changes the susceptibility to alternans of action potential duration (APD) in a rabbit model of chronic myocardial infarction (MI). Optical mapping experiments using voltage-sensitive dyes were performed in 14 rabbit hearts. We found that (1) APD alternans starts at a significantly slower pacing rate in hearts with MI (n=7) than in normal hearts (n=7), with the original sites of alternans of APD located in the infarct region and infarct adjacent regions. (2) Alternans of activation cycle length (CL) precedes the occurrence of spatially discordant alternans of APD, with the regions of activation CL alternans located in the infarct adjacent regions. Based on these results, we conclude that susceptibility to alternans are significantly enhanced in this rabbit model of chronic MI, and the enhancement is strongly correlated to structural and functional heterogeneity imposed by the infarction.**

I. Introduction

Chronic myocardial infarction (MI) is associated with structural discontinuities and functional remodeling in the myocardium. It is still not clear how these changes in the settings of chronic myocardial infarction are related to the alternans of repolarization, which accounts for the T-wave alternans [4] that is recently found to be a reliable predictor for sudden cardiac death after MI [1, 2].

Spatially discordant alternans, which contains neighboring regions with out-of-phase alternans of repolarization, produces large gradient of repolarization to cause conduction block and induce arrhythmia [3]. The top panel of Figure 1 shows typical action potentials of discordant APD alternans (i.e., short-long-short APD sequence (represented by blue) vs. long-short-long APD sequence (represented by red)). As can be seen in the bottom-left panel in Figure 1, regions of discordant alternans were separated by white nodal lines, where the gradient of repolarization can be large enough to produce conduction block and induce reentrant arrhythmia as shown by the activation sequence from blue to red in the bottom-right panel in Figure 1.

Modeling studies have shown that conduction velocity restitution is the underlying mechanism of spatially discordant alternans [4, 5]. Structural discontinuities were also proposed to promote spatially discordant alternans [6]. However, in that study [6], structural barriers were acutely created by argon ion laser and thus were distinct from structural discontinuities in the diseased heart with MI. To further test the role of structural discontinuities in producing spatially discordant alternans, a clinically relevant animal model should be used.

The present study was designed to clarify whether molecular remodeling increases the susceptibility to alternans in the settings of chronic MI, and whether structural discontinuities correlate with spatially discordant alternans. In order to answer these questions, optical action potentials were recorded by high resolution CMOS camera at various pacing rates.

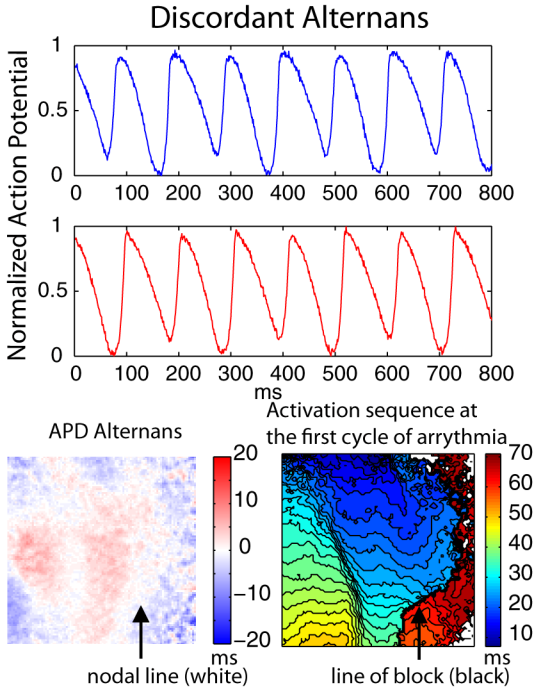

Figure 1. Top panel shows the traces of optical action potentials with discordant action potential duration (APD) alternans, indicated by out-of-phase alternation between long and short APDs. Bottom left panel is a map of APD alternans, amplitude of which is indicated by the intensity of the color. Presence of both red and blue colors indicates occurrence of spatially discordant alternans. A large gradient of repolarization due to spatially discordant alternans along the nodal line (indicated by the arrow in the left) produced conduction block (indicated by the arrow in the right) and initiate arrhythmia, as can be seen in the bottom right panel.

II. Methods and Material

The experimental protocol was approved by the Institutional Animal Care and Use Committee of Washington University. Fourteen New Zealand white rabbits of either sex were used in this study. Seven rabbits

Manuscript received April 7, 2009. Supported by NIH grants R01 HL082729 and R01 HL67322.

Qing Lou is with Washington University, St. Louis, MO 63130 USA; email: ql4@cec.wustl.edu

Igor R. Efimov is with Washington University, St. Louis, MO 63130 USA. email: igor@wustl.edu.

underwent in vivo survival surgery to induce chronic MI via ligation of a descending branch of the left circumflex artery, and other 7 rabbits were not subject to the surgery and were used as controls. Rabbits were allowed to heal for an average of 147±49 days before optical mapping experiments.

Optical Mapping Experiment

Rabbits were injected intravenously with sodium pentobarbital (50 mg/kg) and 1000-2000 U heparin. Hearts were quickly excised, and then Langendorff-perfused with oxygenated Tyrode solution. The excitation contraction uncoupler Blebbistatin (5μM; TOCRIS) was added to the perfusate to suppress motion artifacts in optical recordings. The heart was stained with voltage sensitive dye RH237 (10-20μL of 1mg/ml solution in dimethyl sulfoxide; Molecular Probe). High-resolution optical mapping (100 × 100, 1000 frames/second) was conducted using a CMOS camera (ULTIMA, SciMedia, CA) to measure the optical action potentials.

Experimental Protocol

After staining with RH237, alternans was induced by decremental apical pacing starting at a basic cycle length of 300ms. The pacing interval was decreased by a step of 20ms in the beginning, and was decreased by a step of 10ms after 220ms. The pacing protocol proceeds until the heart cannot be paced or arrhythmia was induced by the pacing.

Data Analysis

Alternans was measured by the difference in APDs between two consecutive beats. The phase was positive for a short-long APD sequence (color coded by red) and was negative for a long-short APD sequence (color coded by blue). Optical APDs were measured at 80% repolarization (APD_{80}). The onset of alternans was measured by the pacing rate at which at least 5% of the optically mapped surface displayed APD alternans > 5ms.

Activation cycle length (CL) is the time between two optical action potential upstrokes. Alternans of activation CLs was measured by the difference in two consecutive activation CLs.

Dynamic APD restitution curves were obtained by plotting APD_{80} against the preceding diastolic interval (DI) for each pacing rate. DI was defined as the time from the 80% repolarization to the next action potential upstroke. The maximum slope of the restitution curve was determined by a linear fit of the steepest portion of the curve.

III. Results

Threshold for APD Alternans

The heart rate threshold for APD alternans is significantly lower in the hearts with MI relative to the normal hearts (285 ± 23 vs. 377 ± 26 beats/min (bpm), Figure 2).

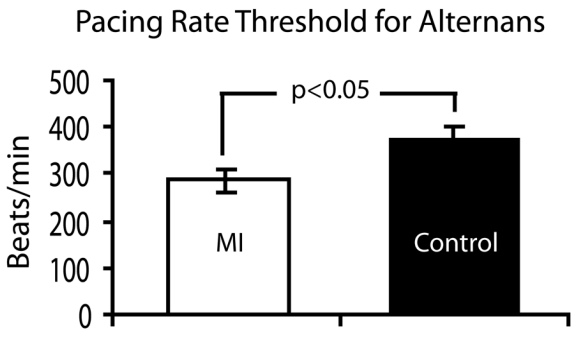

Figure 2. Pacing rate thresholds for alternans in hearts with myocardial infarction (MI) and control hearts.

The alternans starts in the infarct region in three out of seven hearts with MI (Figure 3). In the other four hearts with MI, alternans starts in the infarct adjacent regions close to apex (Figure 4). Spatially discordant alternans was induced in all hearts with MI at a pacing rate of 360 ± 30 bpm, which is significantly lower than 450 ± 63 bpm, which is the threshold of pacing rate for three control hearts with inducible spatially discordant alternans. Spatially discordant alternans could not be induced in other four control hearts, even though they could be paced at an average rate of 434 ± 32 bpm.

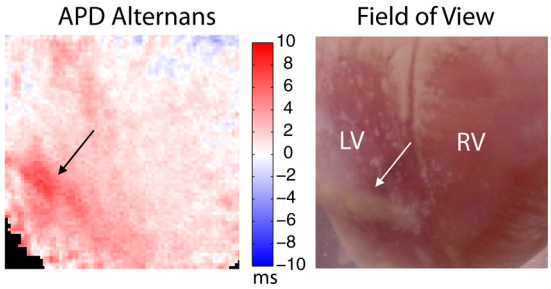

Figure 3. The first site of alternans appears in the infarct region. The black arrow in the left indicates the sites of alternans when the heart was paced at 286 beats/min. Amplitude of alternans is represented by intensity of each color. The white arrow in the right indicates the infarct located in the posterior left ventricle.

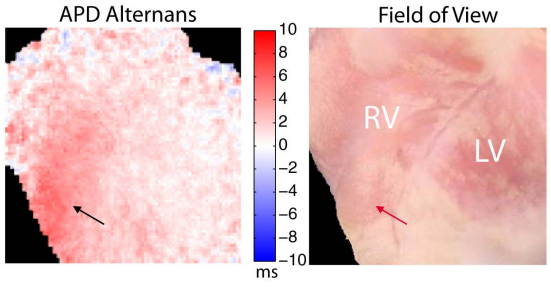

Figure 4. The first site of alternans appears in the infarct adjacent regions. The black arrow in the left indicates the sites of alternans when the heart was paced at 273 beats/min. Amplitude of alternans is represented by intensity of each color. The red arrow in the right indicates the same region pointed out by the black arrow. As can be seen, this region is located adjacent to the white infarct in the apex of both anterior left ventricle and right ventricle.

Activation Cycle Length Alternans and Spatially Discordant Alternans

Figure 5 illustrates a typical observation that activation CL alternans precedes the appearance of spatial discordant alternans. It was obtained in a heart with MI when the basic cycle length of pacing interval was switched from 145ms to 140ms. The top-left panel shows the map of alternans of activation CL alternans plotted from the data acquired right after the switch of pacing rates. The most prominent region of alternans of activation CL is indicated by the dark red area in the apical region next to the infarct. The bottom-left panel is the map of APD alternans obtained from the same data for the top-left panel. The bottom-right panel is also a map of APD alternans but was plotted using the data acquired one minute after the pacing rate change. It can be seen that APD alternans changes from spatial concordant alternans to spatial discordant alternans, which is evident from the presence of both blue and red regions separated by white lines often called nodal lines. Importantly, the dark red region located in top-left panel corresponds well with the blue region at the apical side on the bottom-right panel. This implies that CL alternans next to the infarct region initiates discordant alternans in the same region.

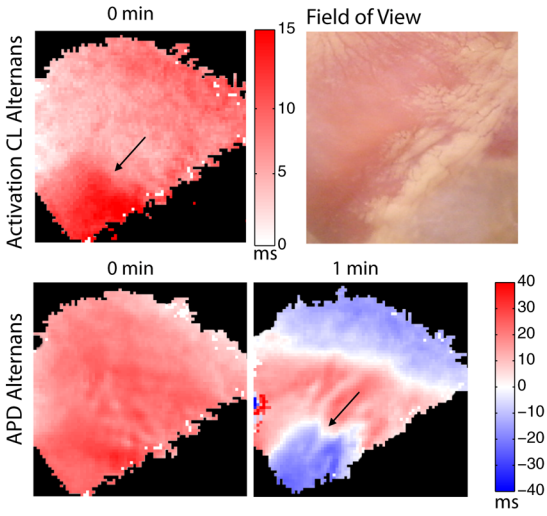

Figure 5. Relation between activation cycle length (CL) alternans and action potential duration (APD) alternans. Two panels on the left column are maps of activation CL alternans (top) and APD alternans (bottom) right after (0 minutes) basic pacing cycle length was changed from 145ms to 140ms. The pattern of APD alternans changed from spatially discordant alternans to spatially discordant alternans after 1 minute, which is shown in the right-bottom panel. It is evident from the region indicated by black arrows that activation CL alternans precedes the appearance of spatially discordant alternans.

APD Restitution

Anatomic location of alternans onset corresponds well with the region with highest maximum slope of the APD restitution curve. Figure 6 shows the color-coded map of maximum slopes of APD restitution curves from the hearts shown in Figure 3. It is evident that the high-slope (slope>1) region corresponds well with the infarction region, and serve as the mechanism to induce APD alternans.

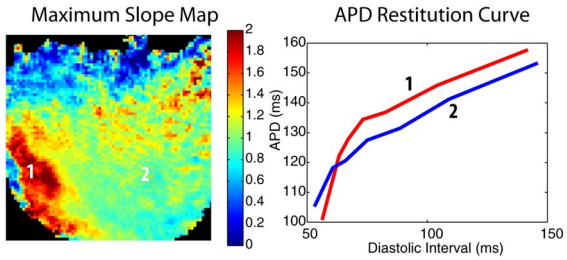

Figure 6. Slopes of APD restitution curve. The left panel is the map of the maximum slopes of APD restitution curve. Two representative APD restitution curve are shown on the right panel with locations indicated by the number. This figure is generated from the same heart in Figure 3. The anatomic site of alternans onset corresponds well with the region of highest slopes.

IV. Discussion

The present study shows that the pacing rate threshold for onset of alternans is significantly decreased in the setting of chronic MI. This can be explained by the large slopes of APD restitution curves in the infarct and infarct adjacent regions. Our results are consistent with the dog study, which shows slopes were larger than 1 in the epicardial border zone where wave breaks occurred [7]. Although APD restitution explains the occurrence of alternans, additional mechanism may also be important. It has been shown that the expression of sarcoplasmic reticulum Ca^{2+} ATPase subtype2a (SERCA2a) and phospholamban, two calcium handling proteins, are significantly reduced in the infarct region and infarct adjacent regions using a sheep model of chronic MI [8]. Reduced SERCA expression was shown to promote both intracellular Ca^{2+} and APD alternans [9]. The role of remodeling in the infarct and infarct adjacent regions is further implicated by the close association of the first site of alternans with the infarct region and infarct adjacent regions.

Our study also shows that alternans of activation CL in the infarct adjacent regions appears first before the occurrence of region of discordant APD alternans. It has been shown in neonatal cell cultures and computer simulations that structural discontinuities changes the property of conduction velocity restitution [10], which creates CL differences [11] and promote spatially discordant alternans [5]. It was also known that the gap junction is remodeled in the infarct boarder zone [12]. And the increased cellular uncoupling due to gap junction remodeling is also likely to facilitate spatially discordant alternans [5, 6].

Limitations of the Study

In this study, only the anterior epicardial surface was mapped. It is possible that some others regions start alternans before the region in our field of view. However, we believe this is unlikely to affect our conclusions.

REFERENCES

[1] T. Ikeda, H. Saito, K. Tanno, H. Shimizu, J. Watanabe, Y. Ohnishi, Y. Kasamaki, and Y. Ozawa, "T-wave alternans as a predictor for sudden cardiac death after myocardial infarction," *Am J Cardiol*, vol. 89, (no. 1), pp. 79-82, Jan 1 2002.

[2] M.J. Mirro, "Strategies for reducing sudden cardiac death: application of microvolt T-wave alternans testing in clinical practice," *Heart Rhythm*, vol. 6, (no. 3 Suppl), pp. S45-8, Mar 2009.

[3] J.M. Pastore, S.D. Girouard, K.R. Laurita, F.G. Akar, and D.S. Rosenbaum, "Mechanism linking T-wave alternans to the genesis of cardiac fibrillation," *Circulation*, vol. 99, (no. 10), pp. 1385-94, Mar 16 1999.

[4] Z. Qu, A. Garfinkel, P.S. Chen, and J.N. Weiss, "Mechanisms of discordant alternans and induction of reentry in simulated cardiac tissue," *Circulation*, vol. 102, (no. 14), pp. 1664-70, Oct 3 2000.

[5] M.A. Watanabe, F.H. Fenton, S.J. Evans, H.M. Hastings, and A. Karma, "Mechanisms for discordant alternans," *J Cardiovasc Electrophysiol*, vol. 12, (no. 2), pp. 196-206, Feb 2001.

[6] J.M. Pastore and D.S. Rosenbaum, "Role of structural barriers in the mechanism of alternans-induced reentry," *Circ Res*, vol. 87, (no. 12), pp. 1157-63, Dec 8 2000.

[7] T. Ohara, K. Ohara, J.M. Cao, M.H. Lee, M.C. Fishbein, W.J. Mandel, P.S. Chen, and H.S. Karagueuzian, "Increased wave break during ventricular fibrillation in the epicardial border zone of hearts with healed myocardial infarction," *Circulation*, vol. 103, (no. 10), pp. 1465-72, Mar 13 2001.

[8] A. Kilic, T. Li, T.D. Nolan, J.R. Nash, S. Li, D.J. Prastein, G. Schwartzbauer, S.L. Moainie, G.K. Yankey, C. DeFilippi, Z. Wu, and B.P. Griffith, "Strain-related regional alterations of calcium-handling proteins in myocardial remodeling," *J Thorac Cardiovasc Surg*, vol. 132, (no. 4), pp. 900-8, Oct 2006.

[9] K.R. Laurita, R. Katra, B. Wible, X. Wan, and M.H. Koo, "Transmural heterogeneity of calcium handling in canine," *Circ Res*, vol. 92, (no. 6), pp. 668-75, Apr 4 2003.

[10] R. Derksen, H.V. van Rijen, R. Wilders, S. Tasseron, R.N. Hauer, W.L. Rutten, and J.M. de Bakker, "Tissue discontinuities affect conduction velocity restitution: a mechanism by which structural barriers may promote wave break," *Circulation*, vol. 108, (no. 7), pp. 882-8, Aug 19 2003.

[11] J.M. Cao, Z. Qu, Y.H. Kim, T.J. Wu, A. Garfinkel, J.N. Weiss, H.S. Karagueuzian, and P.S. Chen, "Spatiotemporal heterogeneity in the induction of ventricular fibrillation by rapid pacing: importance of cardiac restitution properties," *Circ Res*, vol. 84, (no. 11), pp. 1318-31, Jun 11 1999.

[12] N.S. Peters, "Myocardial gap junction organization in ischemia and infarction," *Microsc Res Tech*, vol. 31, (no. 5), pp. 375-86, Aug 1 1995.